Published in final edited form as:
Int J Radiat Oncol Biol Phys. 2008 March 1; 70(3): 816–825. doi:10.1016/j.ijrobp.2007.10.047.

A MITOCHONDRIA-TARGETED NITROXIDE/HEMIGRAMICIDIN S CONJUGATE PROTECTS MOUSE EMBRYONIC CELLS AGAINST GAMMA IRRADIATION

Jianfei Jiang, Ph.D.[*,†], **Natalia A. Belikova, Ph.D.**[*,†], **Adam T. Hoye, B.A.**[*,‡], **Qing Zhao, B.S.**[*,†], **Michael W. Epperly, Ph.D.**[*,§], **Joel S. Greenberger, M.D.**[*,§], **Peter Wipf, Ph.D.**[*,‡], and **Valerian E. Kagan, Ph.D., D.Sci.**[*,†]

[*] *Center for Medical Countermeasures Against Radiation, University of Pittsburgh, Pittsburgh, PA*

[†] *Center for Free Radical and Antioxidant Health, Department of Environmental and Occupational Health, University of Pittsburgh, Pittsburgh, PA*

[‡] *Department of Chemistry, University of Pittsburgh, Pittsburgh, PA*

[§] *Department of Radiation Oncology, University of Pittsburgh, Pittsburgh, PA*

Abstract

Purpose—To evaluate the *in vitro* radioprotective effect of the mitochondria-targeted hemigramicidin S–conjugated 4-amino-2,2,6,6-tetramethyl-piperidine-*N*-oxyl (hemi-GS-TEMPO) 5-125 in γ-irradiated mouse embryonic cells and adenovirus-12 SV40 hybrid virus transformed human bronchial epithelial cells BEAS-2B and explore the mechanisms involved in its radioprotective effect.

Methods and Materials—Cells were incubated with 5-125 before (10 minutes) or after (1 hour) γ-irradiation. Superoxide generation was determined by using dihydroethidium assay, and lipid oxidation was quantitated by using a fluorescence high-performance liquid chromatography–based Amplex Red assay. Apoptosis was characterized by evaluating the accumulation of cytochrome *c* in the cytosol and externalization of phosphatidylserine on the cell surface. Cell survival was measured by means of a clonogenic assay.

Results—Treatment (before and after irradiation) of cells with 5-125 at low concentrations (5, 10, and 20 μM) effectively suppressed γ-irradiation–induced superoxide generation, cardiolipin oxidation, and delayed irradiation–induced apoptosis, evaluated by using cytochrome *c* release and phosphatidylserine externalization. Importantly, treatment with 5-125 increased the clonogenic survival rate of γ-irradiated cells. In addition, 5-125 enhanced and prolonged γ-irradiation–induced G_2/M phase arrest.

Conclusions—Radioprotection/mitigation by hemi-GS-TEMPO likely is caused by its ability to act as an electron scavenger and prevent superoxide generation, attenuate cardiolipin oxidation in mitochondria, and hence prevent the release of proapoptotic factors from mitochondria. Other mechanisms, including cell-cycle arrest at the G_2/M phase, may contribute to the protection.

Reprint requests to: Valerian E. Kagan, Ph.D, D.Sci., Department of Environmental and Occupational Health, University of Pitts-burgh, Bridgeside Point, 100 Technology Drive, Suite 333, Pitts-burgh, PA 15219. Tel: (412) 624-9479; Fax: (412) 624-9361; E-mail: kagan@pitt.edu.

Conflict of interest: none.

Keywords

γ-Irradiation; Hemigramicidin S-conjugated nitroxide; Reactive oxygen species; Cardiolipin oxidation; Cytochrome *c*

INTRODUCTION

The biologic consequences of exposure to ionizing radiation (IR) include genomic instability and cell death (1). It is assumed that radiolytically generated radicals are the primary cause of damage from IR. Direct radiolysis of water and the secondary reactive intermediates with a short lifetime (10^{-10}–10^{-6} seconds) mediate the chemical reactions that trigger the damage of cellular macromolecules, including DNA and proteins, as well as phospholipids in membranes (2). The DNA is believed to be the primary target for the radical attack, resulting in single and double DNA strand breaks (3). To maintain the genomic integrity, multiple pathways of DNA repair and cell-cycle checkpoint control are activated in response to irradiation-induced DNA damage (4). Failure of these repair and regulatory systems leads to genotoxicity, malignant transformation, and cell death (5).

One of the major mechanisms of IR-induced cell death is apoptosis, most commonly realized through a mitochondria-dependent intrinsic pathway (6). The latter includes permeabilization of mitochondria followed by the release of cytochrome (cyt) *c* and other proapoptotic factors (Smac/Diablo [second mitochondrial-derived activator of caspase/direct inhibitor of apoptosis-binding protein with low pI], En-doG [endonuclease G], Omi/HtrA2, and AIF [apoptosis-inducing factor]) into the cytosol as the key events in the execution of the death program. The released cyt *c* facilitates the formation of apoptosomes by interacting with apoptotic protease activating factor 1 (Apaf-1) and then recruits and activates procaspase-9 and triggers the proteolytic cascade that ultimately leads to cell disintegration. Release of proapoptotic factors and caspase activation designate the commencement of irreversible stages of apoptosis. Therefore, significant drug discovery efforts were directed toward the prevention of these events, particularly of the mitochondrial injury representing an important point of no return (7).

However, the exact mechanisms of cyt *c* release from mitochondria are still poorly understood. It was postulated that generation of reactive oxygen species (ROS), likely by means of disrupted electron transport, has a crucial role in promoting cyt *c* release from mitochondria (8). Notably, ROS can induce mitochondria membrane permeabilization both *in vitro* and *in vivo*, and the mitochondrial membrane transition pore was shown to be redox sensitive (9). Conversely, antioxidants and reductants, overexpression of manganese superoxide dismutase (MnSOD) (10), and thioredoxin (11) can delay or inhibit apoptosis.

Previous studies showed that early in apoptosis, a mitochondria-specific phospholipid-cardiolipin (CL) translocated from the inner to the outer mitochondrial membrane and activated cyt *c* into a CL-specific peroxidase (12,13). The activated cyt *c* further catalyzed the oxidation of CL by using mitochondrially generated ROS (13). Most importantly, oxidized CL is an important contributor to the release of cyt *c* from mitochondria (13,14), which might be attributed to changes in microenvironment for the interaction between this phospholipid and cyt *c* (15,16) and/or participation of oxidized CL in the formation of mitochondrial permeability transition pores (MTP) in coordination with Bcl-2 family proteins (Bid, Bax/Bak), as well as adenine nucleotide translocator (ANT) and voltage-dependent anion channel (VDAC) (14, 17). In addition to their essential role in the apoptotic signaling pathway, ROS were also implicated in perpetuation of the bystander effect (18,19) and genomic instability after irradiation exposure (20–22). Hence, elimination of intracellular ROS, particularly its major

source, mitochondrial ROS, by antioxidants may be an important opportunity for developing radioprotectors and radiomitigators. Protection by antioxidants against IR has been studied for more than 50 years (23).

Among different antioxidants, stable nitroxide radicals were suggested as potent radioprotectors because of the multiplicity of their direct radical scavenging properties, as well as catalytic "enzyme"-like mechanisms (24,25). 4-Hydroxy-2,2,6,6-tetramethylpiperidine-*N*-oxyl (TEMPOL) is a nitroxide with properties as a radioprotector *in vitro* and *in vivo* that were studied extensively (26–29). Although found to be effective, the required high millimolar concentrations, partially because of its poor partitioning into cells and mitochondria, set a limit for broader applications of TEM-POL (30). Recent developments in targeted delivery of antioxidants, including nitroxides, to mitochondria offer new opportunities in radioprotection of cells and tissues (31,32). We showed that conjugation of 4-amino-2,2,6,6-tetramethyl-piperidine-*N*-oxyl (4-AT) with a segment of gramicidin S (GS) dramatically increased intracellular and mitochondrial accumulation of the nitroxide conjugates, resulting in decreased levels of mitochondrial superoxide, inhibition of CL peroxidation, and protection of mouse embryonic cells against actinomycin D–induced apoptosis (31,32). Therefore, we hypothesized that mitochondria-targeted hemigramicidin S conjugated 4-amino-2,2,6,6-tetramethyl-piperidine-*N*-oxyl hemi-GS-TEMPO may be effective in protecting cells against IR-induced cell death, thus offering a convenient therapeutic window for radiomitigation. Here, we present evidence that low micromolar concentrations of a hemi-GS-TEMPO homologue, 5-125 (Fig. 1A), effectively protected mouse embryonic cells and human bronchial epithelial BEAS-2B cells against γ-irradiation using preirradiation or postirradiation treatments.

METHODS AND MATERIALS

Materials

The Hemi-GS-TEMPO 5-125 was prepared as previously described (31). Microperoxidase-11 (MP-11), 4-AT, polyethylene glycol-superoxide dismutase (PEG-SOD), and propidium iodide (PI) were from Sigma (St. Louis, MO). Annexin-V kit was from Biovision (Mountain View, CA). Amplex Red (*N*-acetyl-3,7-dihy-droxyphenoxazine) and dihydroethidium (DHE) were purchased from Invitrogen (Carlsbad, CA). Anti-cyt *c* antibody was purchased from BD Pharmingen (San Diego, CA), and antiactin antibody was from Calbiochem (San Diego, CA). All other reagents, unless indicated, were from Sigma.

Cell culture

Mouse embryonic cells (courtesy of Dr. X. Wang, University of Texas, Dallas) were cultured in Dulbecco's Modified Eagle's Medium (DMEM) supplemented with 15% fetal bovine serum, 25 mM of HEPES (4(2-hydroxyethyl)-1-piperazineethane-sulfonic acid), 50 mg/L of uridine, 110 mg l/L of pyruvate, 2 mM of glutamine, 1 × nonessential amino acids, 0.05 mM of 2′-mercaptoethanol, 0.5×10^6 U/L of mouse leukemia inhibitory factor, 100 U/L of penicillin, and 100 μg/L of streptomycin in a humidified atmosphere of 5% carbon dioxide: 95% air at 37°C. The adenovirus-12 SV40 hybrid virus transformed human bronchial epithelial cells BEAS-2B were obtained from American Type Culture Collection (Manassas, VA) and cultured in a serum-free bronchial epithelial growth medium (Clonetics, Walkersville, MD).

Electron paramagnetic resonance-based analysis of partitioning and distribution of nitroxides

To compare partitioning efficiency, cells (1×10^7/ml) were incubated with 10 μM of nitroxides for 10 minutes. EPR spectra of nitroxide radicals in cell or mitochondrial fraction were recorded after mixing with acetonitrile (1:1 vol/vol) after 5 minutes of incubation with 2 mM of $K_3Fe(CN)_6$ using a JEOL-RE1X EPR spectrometer (Joel, Tokyo, Japan) under the following

conditions: 3,350 G center field, 25 G scan range, 0.79 G field modulation, 20 mW microwave power, 0.1 second time constant, and 4 minutes scan time. Mitochondria were obtained by using a mitochondria isolation kit (Pierce, Rockford, IL) according to the manufacturer's instructions. Partitioning efficiency was calculated as percentage of initial signal. Amounts of nitroxide radicals integrated into mitochondria were normalized to the content of cyt *c* oxidase subunit IV(COX-IV).

Irradiation

Cells were cultured in fresh medium before irradiation and were γ-irradiated using a Shepherd model 143–45A irradiator (J.L. Shepherd & Associates, San Fernando, CA) at a dose-rate of 4 Gy/min. Cells were incubated with nitroxides in complete culture medium during preirradiation (10 minutes) or postirradiation (1 hour) treatment. Nitroxides containing medium were replaced with fresh culture medium after the indicated incubation period (2, 3, 4, 5, or 6 hours). Cells were then incubated at 37°C in 5% carbon dioxide until harvest. For comparison, cells were also treated with PEG-SOD (100 U/ml) 10 minutes before irradiation.

Superoxide generation

Oxidation-dependent fluorogenic dye, DHE, was used to evaluate intracellular production of superoxide radicals. The DHE is cell permeable and in the presence of superoxide, is oxidized to fluorescent ethidium, which intercalates into DNA. Briefly, cells were washed once with serum/phenol red–free medium at the indicated time, then incubated with 5 μM of DHE for 30 minutes in serum/phenol red–free medium. At the end of incubation, cells were collected by means of trypsinization and resuspended in phosphate-buffered saline (PBS). The fluorescence of ethidium was measured by using a FACScan flow cytometer (Becton-Dickinson, Rutherford, NJ) supplied with the CellQuest software. Mean fluorescence intensity from 10,000 cells was acquired by using a 585/42-nm band-pass filter.

CL oxidation

The CL hydroperoxides were determined by means of fluorescence high-performance liquid chromatography (HPLC) of products formed in an MP-11–catalyzed reaction with a fluorogenic substrate, Amplex Red. Oxidized phospholipids were hydrolyzed by using pancreatic phospholipase A_2 (2 U/ml) in 25 mM of phosphate buffer containing 1 mM $CaCl_2$, 0.5 mM of EDTA, and 0.5 mM of sodium dodecyl sulfate (pH 8.0 at room temperature for 30 minutes). After that, Amplex Red and MP-11 were added and samples were incubated for 40 minutes at 4°C. A Shimadzu LC-100AT vp HPLC system equipped with fluorescence detector (RF-10Axl, excitation/emission = 560/590 nm) and autosampler (SIL-10AD vp) (Shimadzu, Columbia, MD) were used for analysis of products separated by means of HPLC (Eclipse XDB-C18 column, 5 μm, 150 × 4.6 mm) (Agilent Technologies, Santa Clara, CA). The mobile phase was composed of NaH_2PO_4 (25 mM, pH 7.0)/methanol (60:40 vol/vol).

Accumulation of cyt c in cytosol

Translocation of cyt *c* was examined by using Western blot. At the end of incubation, harvested cells were resuspended in lysis buffer containing 250 mM of sucrose, 20 mM of HEPES-potassium hydroxide (KOH) (pH 7.5), 10 mM of potassium chloride, 1.5 mM of magnesium chloride, 1 mM of ethylene glycol tetraacetic acid (EDTA), 1 mM of EGTA, 1 mM of dithiothrestol (DTT), 1 mM of phenylmethylsulfonyl fluoride (PMSF), 1 μg/ml of aprotinin, 1 μg/ml of leupeptin, and 0.05% digitonin for 3 minutes on ice, then centrifuged at 8,500 × *g* for 5 minutes. The resulting supernatants were subjected to 12% sodium dodecyl sulfate-polyacrylamide gel electrophoresis and transferred to a nitrocellulose membrane, which was probed with antibodies against cyt *c* or actin (loading control), followed by horseradish peroxidase–coupled detection.

Phosphatidylserine externalization

Externalization of phosphatidylserine (PS) was analyzed by means of flow cytometry using an Annexin-V kit. Briefly, harvested cells were stained with Annexin-V–fluorescein isothiocyanate and PI for 5 minutes in the dark before flow cytometry analysis. Ten thousand events were collected on a FACScan flow cytometer (Becton-Dickinson) supplied with CellQuest software.

Clonogenic assay

Cells were plated in 35-mm Petri dishes with 2 ml of culture medium at a proper density (100–1,000 cells/dish). Cells were treated with 5-125 either before (10 minutes) or after (1 hour) γ-irradiation. The Hemi-GS-TEMPO 5-125 was removed from medium 4 hours after irradiation. Colonies were fixed and stained with 0.25% crystal violet and 10% formalin (35% vol/vol) in 80% methanol for 30 minutes after a 9-day incubation period, and colonies of 50 or more cells were counted as survivors. The surviving fraction was calculated as the plating efficiency of samples relative to that of control. Data were fitted to the single-hit multitarget model by using SigmaPlot 9.0 (Systat Software, San Jose, CA). The D_0 values were calculated as the reciprocal of the slope of the exponential region of the survival curves. The measure of the shoulder region (n) is where the exponential region extrapolates to the X axis. Data are presented are mean ± SE ($n = 3$).

DNA content determination

Cellular DNA content was measured through the incorporation of PI. Briefly, cells were fixed with 70% ethanol, then washed with PBS and resuspended in PBS containing 100 μg/ml of DNase-free RNase A (Roche Molecular Biochemicals, Mannheim, Germany) and 40 μg/ml of PI. Cellular DNA content was determined by means of linear amplification in the FL-3 channel (650-nm long-pass filter) of a FACScan flow cytometer equipped with CellQuest software. Cell debris was gated out by forward and side scatter under the same condition, and a minimum of 10,000 gated cells was acquired. Cell counts were plotted against FL-3 area on a linear scale. Histograms from one representative experiment of three are shown. Sub-G1, hyperploid, and G_2/M populations were quantified and expressed as a percentage of the total gated population, and values were averaged from three experiments.

Statistical analysis

All data are expressed as mean ± SE of at least three independent experiments. Statistical comparisons between groups were performed by using Student's t test.

RESULTS

Hemi-GS-TEMPO 5-125 partitions into mitochondria of mouse embryonic cells

We used EPR spectroscopy to evaluate partitioning of 5-125 (Fig. 1A) into cells, particularly into their mitochondrial fraction. A distinctive characteristic signal from the nitroxide moiety of 5-125 was detected in mitochondria (Fig. 1D). Thus, the estimated partitioning of 5-125 into cells and mitochondria was 62.3% and 16.1% of the total, respectively (Fig. 1C). Conversely, greater than 98% of the parental compound 4-AT (Fig. 1B) remained in the aqueous extracellular medium under the same condition. Accordingly, no discernable EPR signal was recorded from mitochondria when cells were incubated with 4-AT (Fig. 1C and 1D).

Hemi-GS-TEMPO 5-125 inhibited γ-irradiation–induced superoxide generation and CL oxidation

To study γ-irradiation–induced oxidative stress and effects of hemi-GS-TEMPO, we used a fluorogenic probe, DHE, for which oxidation to ethidium is believed to be caused

predominantly by the intracellular production of superoxide (33). Gamma-irradiation (10 Gy) induced superoxide generation in mouse embryonic cells in a time-dependent manner (Fig. 2A). Mean fluorescence of ethidium was 1.6- ($p < 0.01$) and 2.5-fold ($p < 0.01$) greater 24 and 48 hours after irradiation compared with nonirradiated controls, respectively. No significant increase in superoxide generation was observed 1 hour after irradiation. Preirradiation (10 minutes) treatment of cells with mitochondria-targeted nitroxide 5-125 (20 μM, removed after 5 hours of postirradiation incubation) dramatically suppressed irradiation-induced superoxide generation ($p < 0.01$; Fig. 2A). Conversely, the nontargeted parental compound, 4-AT, had no effect on γ-irradiation–induced superoxide generation under the same conditions (data not shown). Because intracellular superoxide level did not increase significantly 1 hour after irradiation, we reasoned that postirradiation treatment also might be effective. Postirradiation treatment (20 μM of 5-125 was added to cells 1 hour after irradiation and removed after a 5-hour incubation) also significantly blocked superoxide generation in irradiated cells after 24 and 48 hours of postirradiation incubation ($p < 0.05$ and $p < 0.01$, respectively; Fig. 2A). The efficiency of 5-125 to suppress irradiation-elicited super-oxide was shown further by comparing with the superoxide scavenging activity of PEG-SOD (Fig. 2A). We found that either preirradiation or postirradiation treatment with 5-125 (20 μM) was more effective in suppressing irradiation-induced superoxide generation than PEG-SOD (100 U/ml).

As previously reported (12), generation of superoxide/ROS is critical for oxidation of CL. Therefore, we assessed the effect of 5-125 on the irradiation-induced accumulation of CL hydroperoxides by using an HPLC-based Amplex Red assay. The content of CL-hydroperoxides in nonirradiated cells (13.1 ± 2.9 pmol/nmol CL) increased to 34.6 ± 3.3 ($p < 0.01$) and 84.3 ± 5.8 ($p < 0.01$) pmol/nmol CL 24 and 48 hours postirradiation, approximately 2.6- and ~6.4-fold increases, respectively (Fig. 2B, insert is a typical two-dimensional high performance thin layer chromatography profile). Oxidation of CL did not exert any effect on the overall phospholipid composition of the cells (Table 1). Accumulation of CL hydroperoxides decreased to 18.1 ± 3.8 ($p < 0.05$) and 39.6 ± 4.6 ($p < 0.01$) pmol/nmol CL in 5-125 pre-treated cells after 24 and 48 hours of postirradiation incubation. Importantly, postirradiation (1-hour) treatment of cells with 5-125 (for 5 hours) also suppressed (albeit less effectively than under pretreatment) irradiation-induced accumulation of CL hydroperoxides to 23.8 ± 3.8 ($p < 0.05$) and 55.8 ± 5.9 ($p < 0.01$) pmol/nmol CL after 24 and 48 hours of postirradiation incubation, respectively.

Effect of hemi-GS-TEMPO 5-125 on γ-irradiation–induced apoptosis

Because oxidation of CL participates in the release of proapoptotic factors from mitochondria into the cytosol (12), we next examined whether inhibition of superoxide generation and CL peroxidation was associated with attenuation of γ-irradiation–induced apoptosis. Western blot analysis showed that γ-irradiation (10 Gy) induced a time-dependent release of cyt *c* into the cytosol (Fig. 3A and 3B). Preirradiation treatment of cells with 5-125 (20 μM) inhibited the accumulation of cyt *c* in the cytosolic fraction. In line with data for CL oxidation, postirradiation treatment with 5-125 inhibited cyt *c* release, although to a lesser degree than under the pretreatment protocol (Fig. 3A and 3B).

The antiapoptotic effects of 5-125 were quantitatively studied further by analyzing PS externalization, another hallmark of cell apoptosis occurring downstream of cyt *c* release. Gamma-irradiation induced PS externalization in approximately 25.9% ± 1.1% of mouse embryonic cells 48 hours after irradiation ($p < 0.01$ vs. 1.1% ± 0.3% in nonirradiated controls). The hemi-GS-TEMPO 5-125 (preirradiation treatment) decreased PS externalization in dose- and time-dependent fashions (Fig. 3B and 3C). Postirradiation treatment of cells with 20 μM of 5-125 (for 2, 4, 5, and 6 hours) also protected cells against γ-irradiation–induced PS externalization (Fig. 3C), although not as effectively as the preirradiation treatment.

To provide further evidence for the radioprotective effect of 5-125, we also used human bronchial epithelial BEAS-2B cells. Gamma-irradiation (10 Gy) induced PS externalization in approximately 21.4% ± 2.0% of cells 72 hours after irradiation exposure. Pretreatment (10 minutes before irradiation, removed after 5 hours of incubation) of cells with 5 and 10 μM of 5-125 significantly attenuated γ-irradiation–induced PS externalization (15.6% ± 1.5% and 11.2% ± 1.0%; $p < 0.05$ and $p < 0.01$ vs. irradiated cells without 5-125 treatment, respectively). Similarly, postirradiation treatment (1 hour) with 5-125 decreased irradiation–induced PS externalization in BEAS-2B cells, although to a lesser extent than the preirradiation regimen (Fig. 3E).

Effect of hemi-GS-TEMPO 5-125 on cell survival

Radioprotective effects of 5-125 were examined further by using the clonogenic survival assay. The hemi-GS-TEMPO alone exerted no effect on the plating efficiency of mouse embryonic cells (data not shown). As shown in Fig. 4, pretreatment (10 minutes) of cells with 20 μM of 5-125 (removed after 4 hours of incubation) provided marked protection of cells, shown by the increased D_0 (1.24 ± 0.03 vs. 0.90 ± 0.04; $p < 0.01$), whereas the parental nonconjugated compound, 4-AT, at the same concentration showed no protective effect (data not shown). Significant ($D_0 = 1.07 \pm 0.04$; $p < 0.05$) radioprotection also was afforded by 5-125 when cells were treated with it 1 hour after irradiation, although its action was less effective compared with preirradiation treatment. The shoulder region n value was not significantly different after preirradiation or postirradiation treatment with 5-125 ($n = 4.53 \pm 0.29$ and 4.95 ± 0.35 vs. 5.92 ± 0.38 in irradiated cells without 5-125 treatment, respectively).

Hemi-GS-TEMPO 5-125 prolonged γ-irradiation–induced G_2/M phase arrest

Arrest at specific points of the cell cycle is a universal response to DNA damage in eukaryotic cells. The G_2 cell-cycle checkpoint after DNA damage helps ensure the integrity of the genome (34,35). Previous work showed that nitroxide treatment led to an increased number of cells in the G_2/M phase of the cell cycle (36). Therefore, we evaluated the effect of 5-125 on cell-cycle distribution (Fig. 5). Pronounced G_2/M phase arrest by γ-irradiation (10 Gy) alone was observed as early as 6 hours after irradiation, at which point approximately 65% of cells were found at the G_2/M phase.

After 24 and 32 hours postirradiation, cells were able to partially override the G_2/M block and reentered mitosis. This was documented by the reappearance of a G_1 peak, which was accompanied by a significant increase in hyperploid population (~15.8% and 21.7% at 24 and 32 hours, respectively; $p < 0.01$ vs. control). By 48 hours, the hyperploid population in γ-irradiated cells mounted up to 25.6%. In the presence of 5-125 (pretreatment), enhanced G_2/M accumulation (~90%) was observed 6 hours after irradiation. By 24 and 32 hours, approximately 78.6% and 62.9% of cells remained in the G_2/M phase ($p < 0.01$ vs. irradiated cells without 5-125 treatment). However, a decreased hyperploid population (4.3% and 11.7% at 24 and 32 hours, respectively) was observed. After 48 hours of postirradiation incubation, although significantly fewer apoptotic cells were detected (Fig. 3C), the hyperploid population (21.9%) was not significantly different from that of irradiated cells without 5-125 treatment. Similar results were obtained when treatment with 5-125 was performed 1 hour after irradiation. Conversely, 4-AT did not exert an effect on cell-cycle distribution in irradiated cells under the same conditions (data not shown). In the absence of irradiation exposure, 5-125 alone did not show an effect on cell-cycle distribution.

DISCUSSION

By undergoing one-electron transfer reactions, nitroxides can either be reduced to the corresponding hydroxylamines or oxidized to the corresponding oxoammonium cation species

(2). The former reaction may be associated with scavenging of excessive electrons from the respiratory chain in mitochondria that prevents reduction of molecular oxygen to superoxide. In addition, hydroxylamines also are effective scavengers of several types of highly reactive radical species (2). Because radiolysis of water is associated with the production of both oxidizing and reducing reactive intermediates, nitroxides may be particularly effective in direct scavenging of irradiation-induced radicals attacking biomacromolecules. In line with this, several groups recently reported that TEMPOL-mediated radioprotection was related to the reduced number of DNA double-strand breaks (2,37). However, it is critical that sufficiently high concentrations of nitroxides are achieved at the sites of scavenging of radiation-induced reactive radical species. Unfortunately, these high millimolar concentrations of nitroxides are impractical for the purpose of prevention of irradiation-induced accumulation of reactive radicals. However, irradiation-induced DNA damage and subsequent signaling triggers apoptotic response of mitochondria, which is usually delayed by several hours from the time of the irradiation exposure. Combined with a recently developed strategy of targeted delivery and concentration of antioxidants in mitochondria, this offers a unique new opportunity for using nitroxides not only as radioprotectors, but also as radiomitigators.

Here, we report for the first time that hemi-GS-TEMPO 5-125 at low concentrations (5–20 μM) afforded a marked radioprotective effect in mouse embryonic cells. The effective concentration was almost 1,000-fold less than that of TEMPOL used in previous studies (2). This effect likely is caused, at least in part, by the increased intracellular and intramitochondrial partitioning of hemi-GS-TEMPO.

According to Mitchell *et al.* (2,28), TEMPOL must be present during irradiation to be effective, suggesting that the protective mechanisms involve interaction with short-lived radiolytic intermediates. We found that postirradiation treatment of cells with 5-125 also protected cells against γ-irradiation, clearly pointing to the involvement of mechanisms different from direct scavenging of radiolysis intermediates in the protective effects. A great deal of research indicated that mitochondria are both the primary source and major target of ROS (reviewed in [38]). A disrupted electron transport chain massively generates superoxide radicals originating from damaged mitochondrial complexes I and III. Mitochondrial proteins and DNA, oxidatively modified by ROS, perpetuate the production of increasing concentrations of ROS, thus causing even more cellular damage. More importantly, oxidation of a mitochondria-specific phospholipid, CL, is implicated in the release of proapoptotic factors from mitochondria into cytosol. Thus, a radical scavenging pathway is a likely mechanism of the action of nitroxide insofar as high concentrations of 5-125 accumulated in mitochondria interact with mitochondrial ROS, the generation of which is dependent on intracellular signaling and delayed by several hours from the moment of irradiation damage to DNA. This is in line with our previous findings, showing effective mitochondrial accumulation and proper orientation of 5-125 at the interface of polar and nonpolar compartments of the mitochondria membrane. This membrane topography permits 5-125 to successfully compete with molecular oxygen for electrons from the respiratory carriers, thereby preventing univalent reduction of molecular oxygen to yield superoxide. This interpretation is compatible with the observation that postirradiation treatment with 5-125 showed less protection compared with preirradiation treatment because of the lack of radical scavenging of radiolytic reactive species during irradiation.

It also is possible that 5-125 exerts its protective action through pathways not related to its direct radical scavenging properties, but associated with its ability to affect general redox regulation, particularly at the level of regulation of DNA repair and cell-cycle check points. Suy *et al.* (36) reported that nitroxides caused an increased number of cells in the G_2/M phase of the cell cycle. Cell-cycle checkpoints (G_1/S and G_2/M) are the major genomic surveillance mechanisms regulated in response to DNA damage. Sustained G_2/M phase arrest allows more

time for repair of DNA damage and enhances survival. Increased radiation resistance with a prolonged arrest in G_2/M was documented (39). Conversely, acceleration of G_2/M transition resulted in radiosensitization of cells (40,41). In this study, we found that 5-125 enhanced γ-irradiation–induced accumulation of the G_2/M population and prolonged the G_2/M phase arrest with either preirradiation or postirradiation treatment. Recent work emphasized the importance of redox status as one of the important factors of regulation of DNA repair and cell-cycle arrest (42,43).

Other mechanisms may contribute further to the radioprotective effect of hemi-GS-nitroxides. Our results show that approximately 74.2% of integrated hemi-GS-TEMPO was located outside mitochondria, including the nucleus. Given the high hydrophobicity of hemi-GS-TEMPO (32), it predominantly partitions into membranes. Similar electron-acceptor functions of 5-125 may be realized in the cytoplasmic and nuclear membranes, provided their truncated electron-transport chains (such as the reduced form of nicotinamide-adenine dinucleotide phosphate oxidase/cyt P-450 complexes in endoplasmic reticulum, electron carriers in nuclear and plasma membranes) act as superoxide generators during irradiation-induced apoptosis. Additionally, 5-125 may act as an SOD-mimetic and dismutate superoxide radicals to hydrogen peroxide (24,25). Finally, Suy *et al.* (44) reported that the nontargeted nitroxide, TEMPOL, stimulated the extra cellular signal-regulated kinase (ERK) signaling pathway, which primarily promotes growth and proliferation/survival.

Because mouse embryonic cells, the major model used in this study, have unusual responses to irradiation, such as P53-independent apoptosis and lack of G_1 checkpoint (45), one can assume that results obtained here are not directly applicable to other cell types. However, the significant radio-protective effect of 5-125 observed in BEAS-2B cells suggests that the protective effect is not limited to a specific cell line with unusual characteristics.

Taken together with the data presented in this study, it is reasonable to hypothesize that multiple mechanisms are involved in the radioprotection of 5-125, including scavenging of electrons from respiratory chains, direct interaction with ROS, prevention of superoxide generation, and CL oxidation in mitochondria and redox regulation of the cell cycle.

Acknowledgements

Supported by National Institutes of Health, National Institute of Allergy and Infectious Diseases Grant U19-AI068021 and The Human Frontier Science Program.

References

1. Little JB, Nagasawa H, Pfenning T, et al. Radiation-induced genomic instability: Delayed mutagenic and cytogenetic effects of X rays and alpha particles. Radiat Res 1997;148:299–307. [PubMed: 9339945]
2. Mitchell JB, Russo A, Kuppusamy P, et al. Radiation, radicals, and images. Ann N Y Acad Sci 2000;899:28–43. [PubMed: 10863527]
3. Bryant PE. Enzymatic restriction of mammalian cell DNA: Evidence for double-strand breaks as potentially lethal lesions. Int J Radiat Biol 1985;48:55–60.
4. Elledge SJ. Cell cycle checkpoints: Preventing an identity crisis. Science 1996;274:1664–1672. [PubMed: 8939848]
5. Sachs RK, Chen AM, Brenner DJ. Proximity effects in the production of chromosome aberrations by ionizing radiation. Int J Radiat Biol 1997;71:1–19. [PubMed: 9020958]
6. Newton K, Strasser A. Ionizing radiation and chemotherapeutic drugs induce apoptosis in lymphocytes in the absence of Fas or FADD/MORT1 signaling. Implications for cancer therapy. J Exp Med 2000;191:195–200. [PubMed: 10620618]

7. Szewczyk A, Wojtczak L. Mitochondria as a pharmacological target. Pharmacol Rev 2002;54:101–127. [PubMed: 11870261]
8. Kowaltowski AJ, Castilho RF, Vercesi AE. Opening of the mitochondrial permeability transition pore by uncoupling or inorganic phosphate in the presence of Ca^{2+} is dependent on mitochondrial-generated reactive oxygen species. FEBS Lett 1996;378:150–152. [PubMed: 8549822]
9. Kroemer G, Reed JC. Mitochondrial control of cell death. Nat Med 2000;6:513–519. [PubMed: 10802706]
10. Wong GH, Elwell JH, Oberley LW, et al. Manganous superoxide dismutase is essential for cellular resistance to cytotoxicity of tumor necrosis factor. Cell 1989;58:923–931. [PubMed: 2476237]
11. Iwata S, Hori T, Sato N, et al. Adult T cell leukemia (ATL)-derived factor/human thioredoxin prevents apoptosis of lymphoid cells induced by L-cystine and glutathione depletion: Possible involvement of thiol-mediated redox regulation in apoptosis caused by pro-oxidant state. J Immunol 1997;158:3108–3117. [PubMed: 9120263]
12. Fernandez MG, Troiano L, Moretti L, et al. Early changes in intramitochondrial cardiolipin distribution during apoptosis. Cell Growth Differ 2002;13:449–455. [PubMed: 12354754]
13. Kagan VE, Tyurin VA, Jiang J, et al. Cytochrome *c* acts as a cardiolipin oxygenase required for release of proapoptotic factors. Nat Chem Biol 2005;1:223–232. [PubMed: 16408039]
14. Petrosillo G, Casanova G, Matera M, et al. Interaction of peroxidized cardiolipin with rat-heart mitochondrial membranes: Induction of permeability transition and cytochrome c release. FEBS Lett 2006;580:6311–6316. [PubMed: 17083938]
15. Ott M, Robertson JD, Gogvadze V, et al. Cytochrome *c* release from mitochondria proceeds by a two-step process. Proc Natl Acad Sci U S A 2002;99:1259–1263. [PubMed: 11818574]
16. Garrido C, Galluzzi L, Brunet M, et al. Mechanisms of cytochrome *c* release from mitochondria. Cell Death Differ 2006;13:1423–1433. [PubMed: 16676004]
17. Gonzalvez F, Gottlieb E. Cardiolipin: Setting the beat of apoptosis. Apoptosis 2007;12:877–885. [PubMed: 17294083]
18. Narayanan PK, Goodwin EH, Lehnert BE. Alpha particles initiate biological production of superoxide anions and hydrogen peroxide in human cells. Cancer Res 1997;57:3963–3971. [PubMed: 9307280]
19. Iyer R, Lehnert BE. Factors underlying the cell growth-related bystander responses to alpha particles. Cancer Res 2000;60:1290–1298. [PubMed: 10728689]
20. Spitz DR, Azzam EI, Li JJ, et al. Metabolic oxidation/reduction reactions and cellular responses to ionizing radiation: A unifying concept in stress response biology. Cancer Metastasis Rev 2004;23:311–322. [PubMed: 15197331]
21. Limoli CL, Giedzinski E, Morgan WF, et al. Persistent oxidative stress in chromosomally unstable cells. Cancer Res 2003;63:3107–3111. [PubMed: 12810636]
22. Kim GJ, Chandrasekaran K, Morgan WF. Mitochondrial dysfunction, persistently elevated levels of reactive oxygen species and radiation-induced genomic instability: A review. Mutagenesis 2006;21:361–367. [PubMed: 17065161]
23. Weiss JF, Landauer MR. Radioprotection by antioxidants. Ann N Y Acad Sci 2000;899:44–60. [PubMed: 10863528]
24. Saito K, Takeshita K, Ueda J, et al. Two reaction sites of a spin label, TEMPOL (4-hydroxy-2,2,6,6-tetramethylpiperidine-*N*-oxyl), with hydroxyl radical. J Pharm Sci 2003;92:275–280. [PubMed: 12532377]
25. Mitchell JB, Samuni A, Krishna MC, et al. Biologically active metal-independent superoxide dismutase mimics. Biochemistry 1990;29:2802–2807. [PubMed: 2161256]
26. Mitchell JB, Krishna MC. Nitroxides as radiation protectors. Mil Med 2002;167:49–50. [PubMed: 11873514]
27. Hahn SM, DeLuca AM, Coffin D, et al. *In vivo* radioprotection and effects on blood pressure of the stable free radical nitroxides. Int J Radiat Oncol Biol Phys 1998;42:839–842. [PubMed: 9845107]
28. Mitchell JB, DeGraff W, Kaufman D, et al. Inhibition of oxygen-dependent radiation-induced damage by the nitroxide superoxide dismutase mimic, tempol. Arch Biochem Biophys 1991;289:62–70. [PubMed: 1654848]

29. Hahn SM, Tochner Z, Krishna CM, et al. Tempol, a stable free radical, is a novel murine radiation protector. Cancer Res 1992;52:1750–1753. [PubMed: 1551104]
30. Gariboldi MB, Ravizza R, Petterino C, et al. Study of in vitro and in vivo effects of the piperidine nitroxide Tempol—A potential new therapeutic agent for gliomas. Eur J Cancer 2003;39:829–837. [PubMed: 12651210]
31. Wipf P, Xiao J, Jiang J, et al. Mitochondrial targeting of selective electron scavengers: Synthesis and biological analysis of hemigramicidin-TEMPO conjugates. J Am Chem Soc 2005;127:12460–12461. [PubMed: 16144372]
32. Jiang J, Kurnikov I, Belikova NA, et al. Structural requirements for optimized delivery, inhibition of oxidative stress and anti-apoptotic activity of targeted nitroxides. J Pharmacol Exp Ther 2006;320:1050–1060. [PubMed: 17179468]
33. Rothe G, Valet G. Flow cytometric analysis of respiratory burst activity in phagocytes with hydroethidine and 2′,7′-dichlorofluorescin. J Leukoc Biol 1990;47:440–448. [PubMed: 2159514]
34. Hartwell LH, Kastan MB. Cell cycle control and cancer. Science 1994;266:1821–1828. [PubMed: 7997877]
35. Featherstone C, Jackson SP. DNA double-strand break repair. Curr Biol 1999;9:R759–R761. [PubMed: 10531043]
36. Suy S, Mitchell JB, Samuni A, et al. Nitroxide tempo, a small molecule, induces apoptosis in prostate carcinoma cells and suppresses tumor growth in athymic mice. Cancer 2005;103:1302–1313. [PubMed: 15685617]
37. Erker L, Schubert R, Yakushiji H, et al. Cancer chemoprevention by the antioxidant tempol acts partially via the p53 tumor suppressor. Hum Mol Genet 2005;14:1699–1708. [PubMed: 15888486]
38. Orrenius S. Reactive oxygen species in mitochondria-mediated cell death. Drug Metab Rev 2007;39:443–455. [PubMed: 17786631]
39. Miyata H, Doki Y, Yamamoto H, et al. Overexpression of CDC25B overrides radiation-induced G_2-M arrest and results in increased apoptosis in esophageal cancer cells. Cancer Res 2001;61:3188–3193. [PubMed: 11306507]
40. Bache M, Pigorsch S, Dunst J, et al. Loss of G_2/M arrest correlates with radiosensitization in two human sarcoma cell lines with mutant p53. Int J Cancer 2001;96:110–117. [PubMed: 11291094]
41. Miyata H, Doki Y, Shiozaki H, et al. CDC25B and p53 are independently implicated in radiation sensitivity for human esophageal cancers. Clin Cancer Res 2000;6:4859–4865. [PubMed: 11156245]
42. Rothstein EC, Lucchesi PA. Redox control of the cell cycle: A radical encounter. Antioxid Redox Signal 2005;7:701–703. [PubMed: 15890015]
43. Cakir Y, Ballinger SW. Reactive species-mediated regulation of cell signaling and the cell cycle: The role of MAPK. Antioxid Redox Signal 2005;7:726–740. [PubMed: 15890019]
44. Suy S, Mitchell JB, Ehleiter D, et al. Nitroxides tempol and tempo induce divergent signal transduction pathways in MDA-MB 231 breast cancer cells. J Biol Chem 1998;273:17871–17878. [PubMed: 9651392]
45. Aladjem MI, Spike BT, Rodewald LW, et al. ES cells do not activate p53-dependent stress responses and undergo p53-independent apoptosis in response to DNA damage. Curr Biol 1998;8:145–155. [PubMed: 9443911]

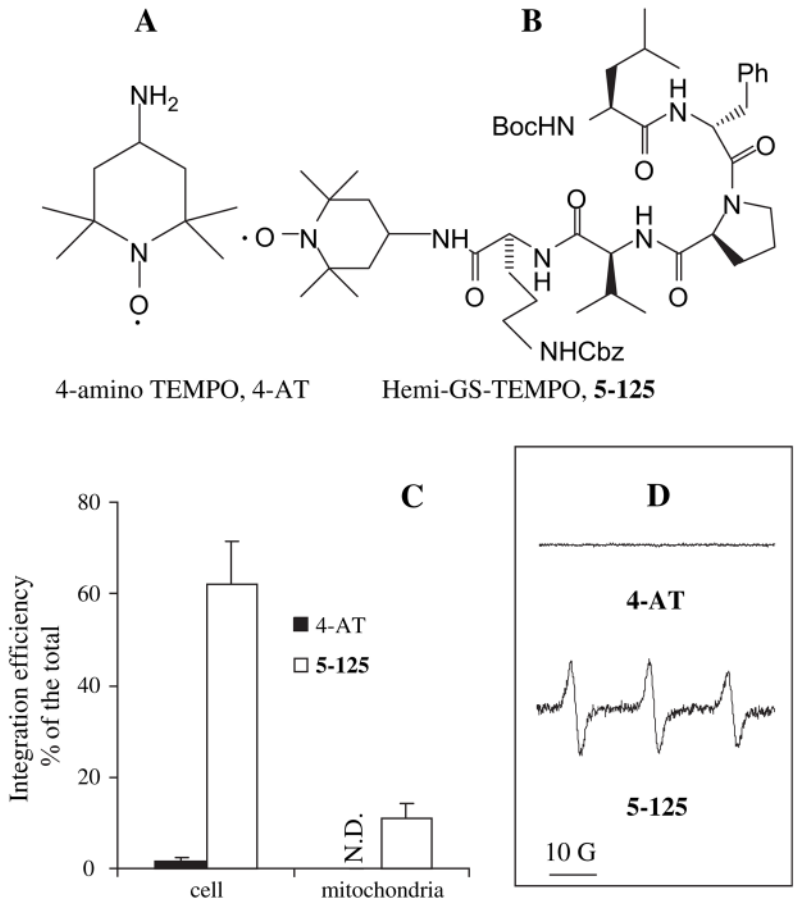

Fig. 1.

Structure of (A) 4-amino-2,2,6,6-tetramethyl-piperidine-*N*-oxyl (4-AT), (B) hemigramicidin S–conjugated 4-amino-2,2,6,6-tetramethyl-piperidine-*N*-oxyl (hemi-GS-TEMPO) 5-125, (C) their cellular and mitochondrial integration efficiencies in mouse embryonic cells, and (D) representative electron paramagnetic resonance (EPR) spectrum of nitroxides recovered from mitochondria.

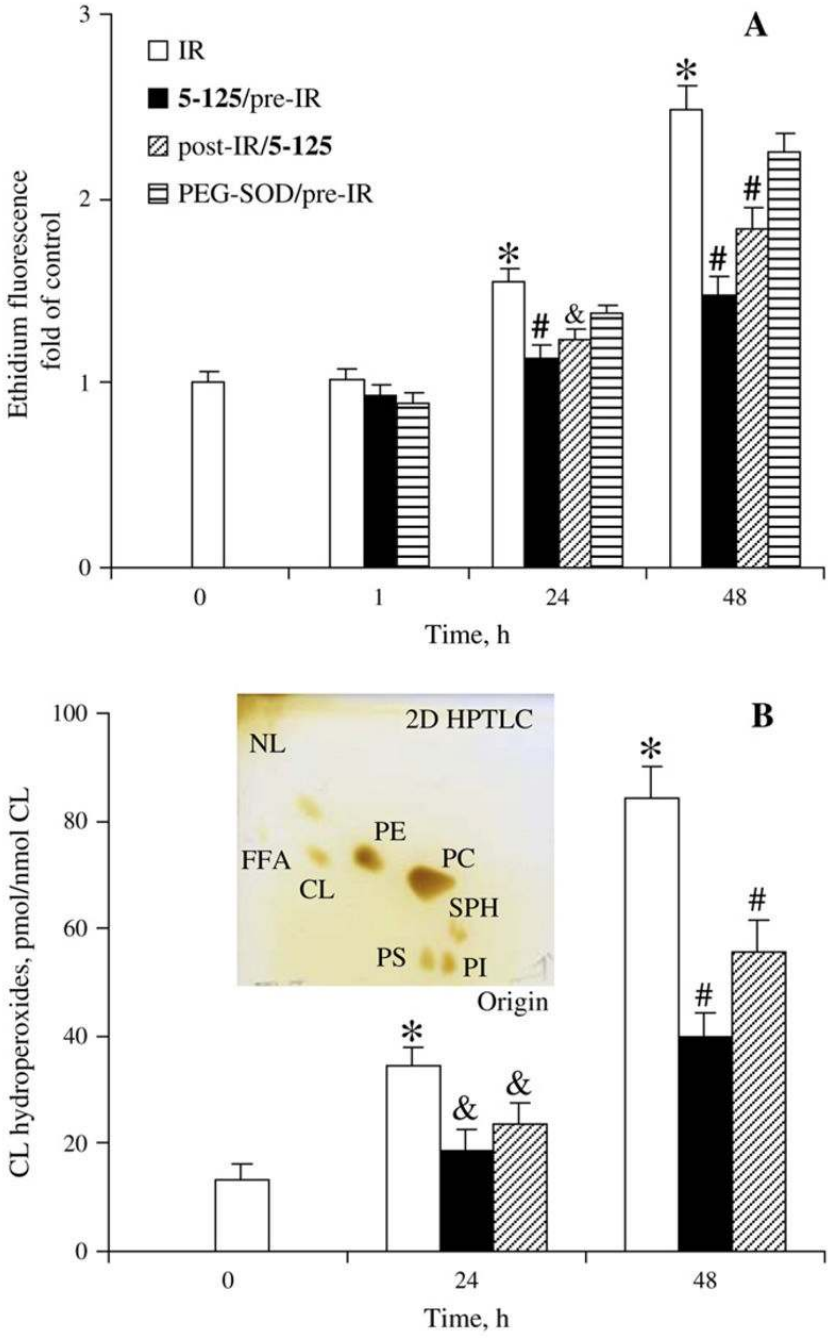

Fig. 2.

Hemigramicidin S–conjugated 4-amino-2,2,6,6-tetra-methyl-piperidine-*N*-oxyl (hemi-GS-TEMPO) 5-125 inhibits γ–irradiation induced (A) superoxide generation. Mouse embryonic cells were exposed to 10 Gy of γ-irradiation. The hemi-GS-TEMPO (20 μM) was added to cells either 10 minutes before or 1 hour after irradiation and removed after 5 hours of incubation. For comparison, cells were incubated with 100 U/ml of polyethylene glycol-superox-ide dismutase (PEG-SOD) 10 minutes before irradiation. Cells were incubated with 5 μM of dihydroethidium (DHE) for 30 minutes at the indicated times. Ethidium fluorescence was analyzed by using a FACScan flow cytometer supplied with CellQuest software. Mean fluorescence intensity from 10,000 cells was acquired by using a 585-nm band-pass filter. (B)

Cardiolipin oxidation. Cardiolipin hydroperoxides were determined by using a fluorescent high-performance liquid chromatography (HPLC)-based Amplex Red assay. Data presented as mean ± SE ($n = 3$). *$p < 0.01$ vs. nonirradiated cells; # (&)$p < 0.01$ (0.05) vs. irradiated cells without 5-125 treatment under the same condition. Insert is a typical 2D-high performance thin layer chromatography profile of phospholipids from cells.

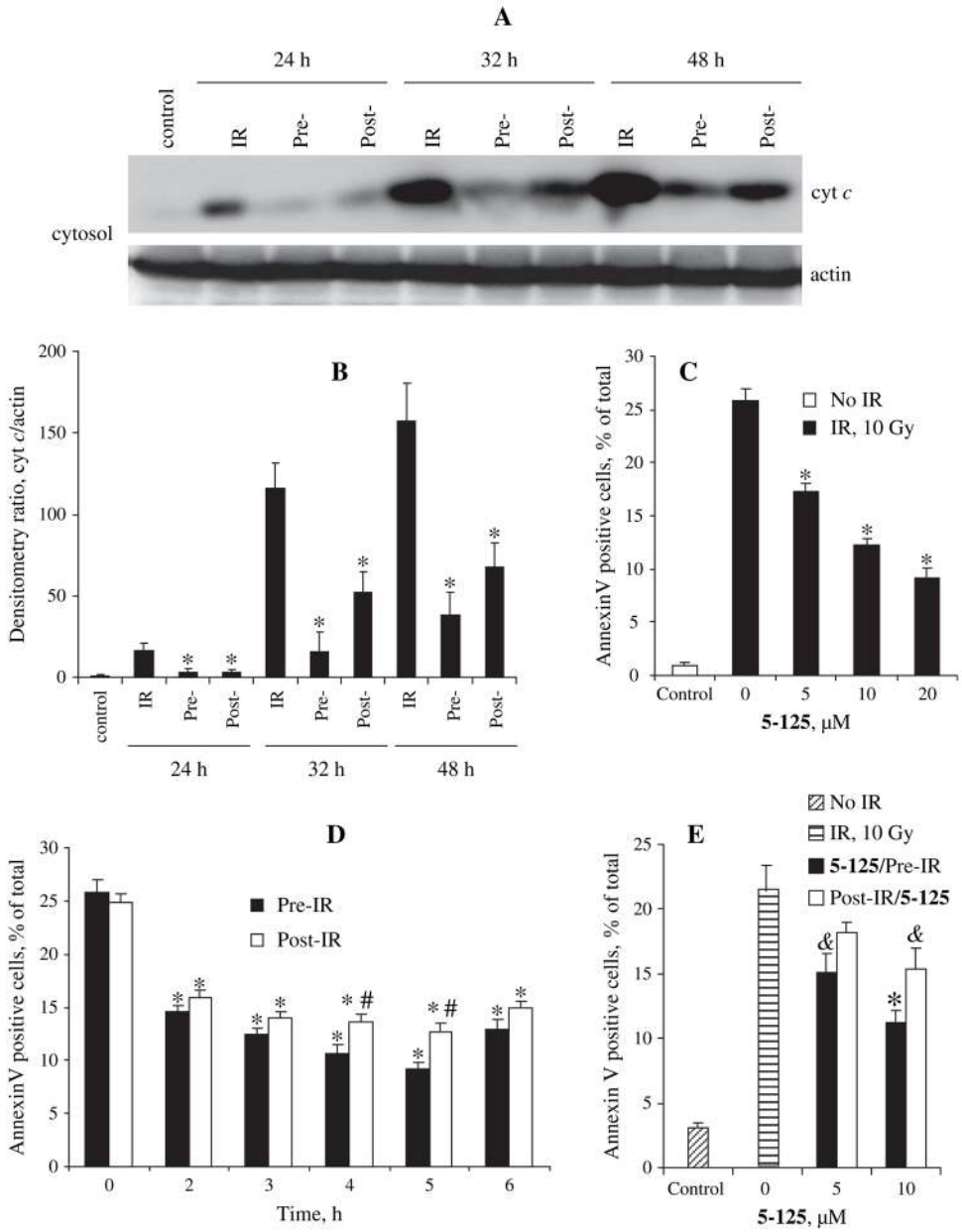

Fig. 3.

(A) Hemigramicidin S–conjugated 4-amino-2,2,6,6-tetramethyl-piperidine-*N*-oxyl (hemi-GS-TEMPO) 5-125 blocks γ-irradiation–induced accumulation of cytochrome (cyt) *c* in the cytosol of mouse embryonic cells. (B) Densitometry ratio of cyt *c*/actin. Semiquantitation of the bands was carried out by means of densitometry using Labworks Image Acquisition and Analysis Software (UVP, Upland, CA). Level of cyt *c* release was expressed as the mean densitometry ratio of cyt *c* over actin. (C) Dose (5, 10, and 20 μM)-dependent radioprotective effect of 5-125 (pretreatment) on γ-irradiation (10 Gy)-induced phosphatidylserine (PS) externalization. After 48 hours of postirradiation incubation, cells were harvested and stained with Annexin-V–fluorescein isothiocyanate (FITC) and propidium iodide (PI) before flow cytometry analysis. (D) Time (2, 3, 4, 5, and 6 hours)-dependent radioprotective effect of 5-125 (20 μM) on γ-irradiation (10 Gy)-induced PS externalization (48 hours after irradiation) in mouse embryonic cells. (E) Effect of 5-125 on γ-irradiation (10 Gy)-induced PS externalization in BEAS-2B

cells. Cells were treated with 5-125 (5 or 10 μM) before (10 minutes) or after (1 hour) irradiation. Externalization of PS was analyzed 72 hours after irradiation exposure. Data shown as mean ± SE ($n = 3$). *(&)$p < 0.01$ (0.05) vs. irradiated cells without 5-125 treatment, #$p < 0.05$ vs. cells pretreated with 5-125.

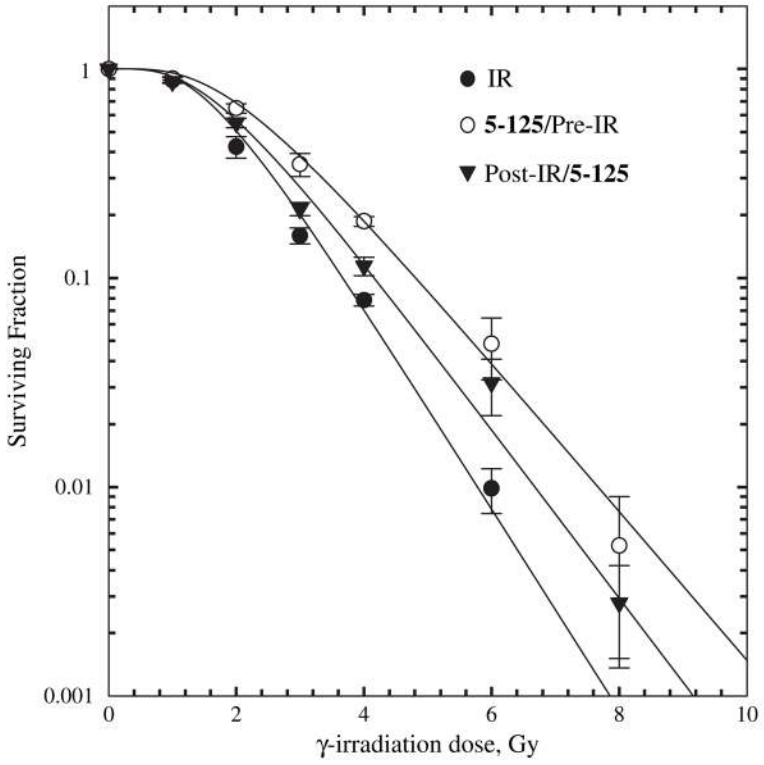

Fig. 4.

Gamma-irradiation dose survival curves of mouse embryonic cells. Cells were pretreated (10 minutes) or post-treated (1 hour) with 5-125 (20 μM), which was removed after a 4-hour incubation period. The surviving fraction was calculated as the plating efficiency of the samples relative to that of the control. Data were fitted to a single-hit multitarget model using SigmaPlot 9.0 (Systat Software). Data presented as mean ± SE (n = 3).

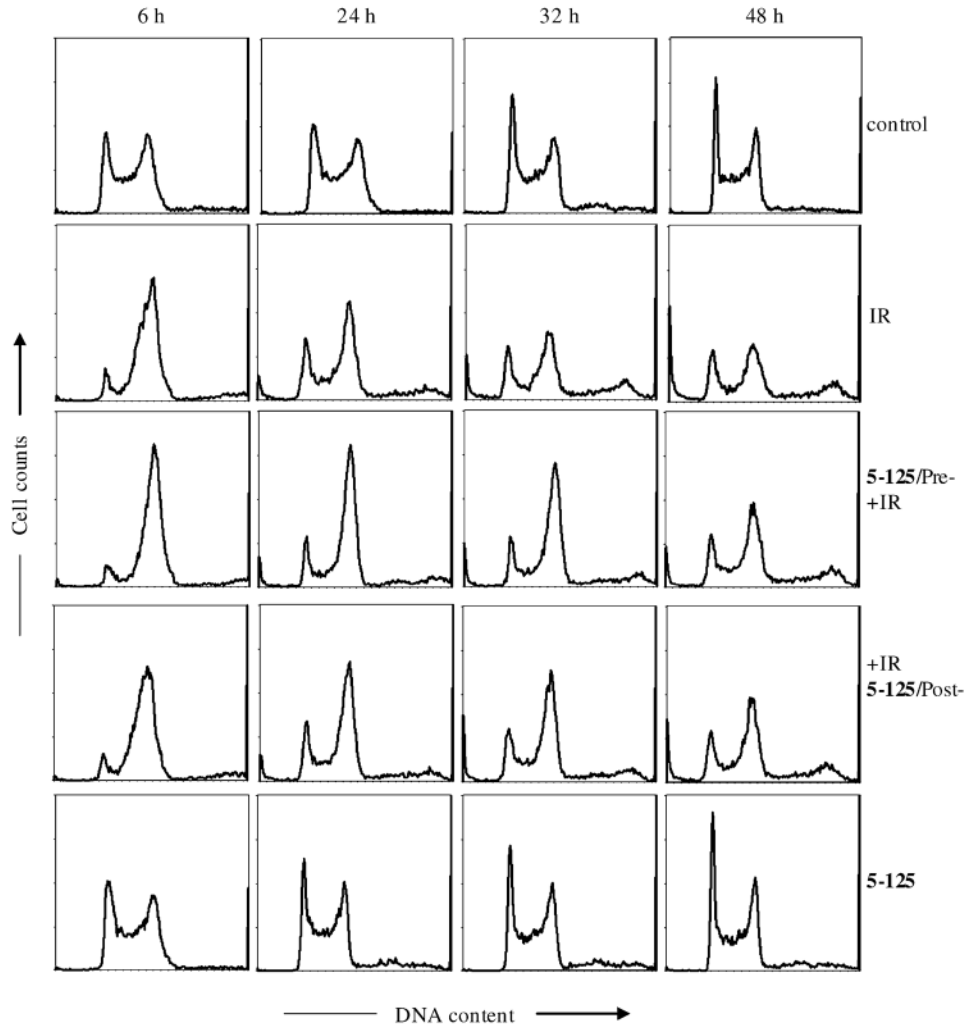

Fig. 5.

Hemigramicidin S–conjugated 4-amino-2,2,6,6-tetramethyl-piperidine-*N*-oxyl (hemi-GS-TEMPO) 5-125 (20 μM) prolongs γ-irradiation (10 Gy)–induced G_2/M arrest in mouse embryonic cells. Harvested cells were fixed in 70% alcohol at 4°C overnight, then pelleted and resuspended in phosphate-buffered saline (PBS) containing 100 μg/ml of RNase A and 40 μg/ml of propidium iodide (PI) for 15 minutes. Cellular DNA content was determined by means of linear amplification in the FL-3 channel (>650 nm) of a FACScan flow cytometer equipped with CellQuest software. Cell debris was gated out by forward and side scatter under the same condition, and a minimum of 10,000 gated cells was acquired. Histograms shown are from one representative experiment of three.

Table 1

Phospholipid composition of mouse embryonic cells

	Phospholipids (% of total)					
	CL	**PC**	**PE**	**PI**	**PS**	**SPH**
Control	1.5 ± 0.1	64.2 ± 2.7	18.8 ± 0.8	6.7 ± 0.4	5.4 ± 0.3	3.4 ± 0.3
IR	1.4 ± 0.1	62.9 ± 3.6	21.4 ± 1.0	6.1 ± 0.4	4.9 ± 0.3	3.3 ± 0.2
5-125/pre-	1.4 ± 0.1	63.7 ± 2.8	19.3 ± 1.1	6.8 ± 0.3	5.2 ± 0.4	3.6 ± 0.2
5-125/post-	1.5 ± 0.1	64.1 ± 3.2	19.1 ± 1.1	6.6 ± 0.3	5.3 ± 0.4	3.4 ± 0.3

Abbreviations: CL = cardiolipin; PC = phosphatidylcholine; PE = phosphatidylethanolamine; PI = phosphatidylinositol; PS = phosphatidyl-serine; SPH = sphingomyelin.

Cells were harvested 24 hours after γ-irradiation. Phospholipids were extracted and then resolved by using 2D-high performance thin layer chromatography. Data expressed as mean ± SE (n = 3).